ICES REPORT 17-13

June 2017

Adaptive Numerical Homogenization for Non-Linear Multiphase Flow and Transport

by

Gurpreet Singh, Yerlan Amanbek, and Mary F. Wheeler

The Institute for Computational Engineering and Sciences
The University of Texas at Austin
Austin, Texas 78712

Reference: Gurpreet Singh, Yerlan Amanbek, and Mary F. Wheeler, "Adaptive Numerical Homogenization for Non-Linear Multiphase Flow and Transport," ICES REPORT 17-13, The Institute for Computational Engineering and Sciences, The University of Texas at Austin, June 2017.

Adaptive Numerical Homogenization for Non-linear Multiphase Flow and Transport

Gurpreet Singh* Yerlan Amanbek Mary F. Wheeler

June 20, 2017

Abstract

One of the major objectives in the development of upscaling approaches is to reduce the computational costs associated with solving fine scale flow and transport problems in heterogeneous porous media. This is due to the availability of reservoir rock property data at fine spatial scales, such as facies distributions, obtained from geological models and field data from well logs. The data sets from each of these sources are themselves at different spatial scales which further adds to the computational challenge. The upscaling approach must not only accommodate these disparate data sets but also capture the flow physics accurately while maintaining computational efficiency. We present a novel upscaling approach which draws upon previous developments of two-scale homogenization [4] to obtain coarse scale properties in addition to dynamic mesh refinement using an enhanced velocity mixed finite element method (EV MFEM) [27]. A transient region is defined where changes in saturation/concentration are above a chosen threshold compared to a non-transient region where these are relatively small. Since most of the recovery technologies employed in oil and gas field operations involve flooding the subsurface porous medium; as in the case of water-flooding, chemical or gas enhanced oil recovery (EOR), these aforementioned transient regions are usually restricted to much smaller subdomains of the entire reservoir domain. The computational efficiency is achieved by using coarse scale parameters, from numerical homogenization, in the non-transient region. Furthermore, the solution accuracy is preserved by using fine scale information only in the transient region. The numerical results section shows that our adaptive homogenization approach closely captures fine scale flow and transport features while maintaining a computational speedup of approximately 4 times for a variety of permeability distributions extracted from the SPE 10 comparative upscaling project [13].

Keywords. enhanced velocity, numerical homogenization, adaptive mesh refinement, multiscale methods, multiphase flow

Abstract

One of the major objectives in the development of upscaling approaches is to reduce the computational costs associated with solving fine scale flow and transport problems in heterogeneous porous media. This is due to the availability of reservoir rock property data at fine spatial scales, such as facies distributions, obtained from geological models and field data from well logs. The data sets from each of these sources are themselves at different spatial scales which further adds to the computational challenge. The upscaling approach must not only accommodate these disparate

data sets but also capture the flow physics accurately while maintaining computational efficiency. We present a novel upscaling approach which draws upon previous developments of two-scale homogenization [4] to obtain coarse scale properties in addition to dynamic mesh refinement using an enhanced velocity mixed finite element method (EV MFEM) [27]. A transient region is defined where changes in saturation/concentration are above a chosen threshold compared to a non-transient region where these are relatively small. Since most of the recovery technologies employed in oil and gas field operations involve flooding the subsurface porous medium; as in the case of water-flooding, chemical or gas enhanced oil recovery (EOR), these aforementioned transient regions are usually restricted to much smaller subdomains of the entire reservoir domain. The computational efficiency is achieved by using coarse scale parameters, from numerical homogenization, in the non-transient region. Furthermore, the solution accuracy is preserved by using fine scale information only in the transient region. The numerical results section shows that our adaptive homogenization approach closely captures fine scale flow and transport features while maintaining a computational speedup of approximately 4 times for a variety of permeability distributions extracted from the SPE 10 comparative upscaling project [13].

1 Introduction

Since the advent of numerical reservoir simulations, oil-field operations have received a substantial boost in confidently predicting recovery estimates and determining operational choices during the deployment of a specific recovery technology. During the screening stage, numerical reservoir models are built and simulations are run to determine feasibility of a number of injection/production scenarios. This requires that the reservoir simulation to be both accurate and time efficient. Furthermore, for an oil and gas reservoir already in production, it is necessary to determine reservoir parameters (permeability, porosity, etc.) with increasing certainty. As the field matures, more efficient practices such as production stimulation, chemical treatment, or infill drilling can substantially increase the life of the reservoir and consequently the overall recovery. Uncertainty quantification (UQ) and parameter estimation have been used extensively in this respect to predict reservoir parameters incorporating well logs, production data and geological models during history matching. These frameworks either rely upon proxy models; which approximate the flow physics in the reservoir, or a field scale reservoir simulator as the forward model or the driving engine for generating multiple realizations. The proxy models often suffer from inadequate representation of flow physics for example, a single phase flow model is often used as a proxy for more involved fluid description such as gas flooding that necessitates an equation of state (EOS) compositional flow model. However, at the other end using a full-field reservoir simulator is prohibitively expensive since the number of realizations; required by UQ and parameter estimation from a reservoir simulator, are of the order of 100 [25]. Additionally, the field data is usually available at different spatial scale due to differences in observations techniques. For example, for well-logs this spatial scale is a few feet whereas data inferred from seismic recordings is usually of the order of 100 feet.

All of these aforementioned challenges prove to be prohibitive for direct numerical simulation of reservoirs. Several upscaling approaches have been developed and are used in the oil and gas industry as well as other porous media communities to reduce the computational costs. These approaches share a common aspect in that they rely upon calculating effective reservoir parameters at some coarse scale, given fine scale parameters. An extensive amount of literature can be found in multiple disciplines (engineering, computational science, and applied mathematics) where these

approaches [19, 6, 7, 16, 28] are interchangeably named as homogenization, upscaling or mass conservative projection. All of these address the multiscale (fine and coarse scale) nature of the problem and the data at hand giving rise to an array of upscaling approaches.

Two-scale homogenization theory is a mathematically consistent, theoretical framework that has been used by several others [2, 23, 21, 9, 4] to derive effective equations for a variety of problems. For a reservoir domain characterized by a length scale L, two-scale homogenization theory makes basic assumptions: (1) existence of an identifiable Representative Elementary Volume (REV) (or a period) with a characteristic length scale l, and (2) a scale separation between these aforementioned two length scale or $\varepsilon = l/L << 1$. The first assumption effectively means that a parameter or reservoir property that oscillates at the fine spatial scale ceases to do so at some coarse spatial scale. Figure 1 shows variation in permeability along a spatial dimension and the REV length scale at which the permeability values cease to oscillate. Although, shown here only for permeability the concept of REV extends to other pertinent reservoir rock properties such as porosity. The second assumption ensures that the problems at the coarse and fine scale can be decoupled so as to obtain effective properties that are independent of the fine scale variations. For further details regarding homogenization theory; both rigorous and formal, the reader is referred to [3] and the citations therein.

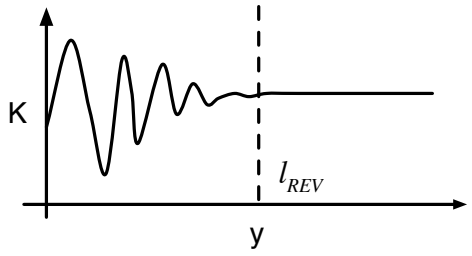

Figure 1: Fine scale permeability variation and the notion of REV; adapted from [8].

We propose an adaptive homogenization approach using local numerical homogenization to reduce computational costs. Here, we use the formal two-scale homogenization framework to derive effective equation at the coarse scale for a given fine scale flow model formulation. Further combined with adaptive mesh refinement (AMR) using EV MFEM [27, 26] to accurately recover fine scale flow features at the saturation front as an upscaling approach. Our approach shares similarities with the adaptive [14] and hybrid [1] multiscale methods in that some form of local enrichment is performed at the saturation front. These latter approaches rely upon enriching local multiscale basis functions as opposed to our approach of local mesh refinement in the region of interest. Although similar, extension of these multiscale approaches to more involved fluid flow description such as EOS compositional flow is not yet clear. Furthermore, the computational overheads in re-evaluating these multiscale basis functions; for non-linear flow and transport problems, might undermine the overall computational efficiency. In this respect, our adaptive homogenization approach poses no such issues and can be easily extended to different flow systems of particular interest to the oil and gas industry such as oil-water, black-oil, and compositional flow for both gas and chemical flooding. Further, an interesting point to note is that homogenization theory clearly indicates that upscaling approaches developed for single-phase flow models cannot be directly applied to more involved

multiphase, multicomponent flow and transport models. For example, the effective equations for two-phase flow model [10]; at the coarse scale, obtained using homogenization differ quite substantially from those of a single-phase flow model [4]. This warrants that the upscaling approach must be altered as the flow models under consideration change. However, the two upscaling approaches do share common elements that are independent of the flow model under consideration. The adaptive homogenization approach proposed here exploits these common elements to render our upscaling approach process independency to some extent.

The structure of this paper is as follows: the model formulation first outlines the two-phase, slightly compressible oil-water flow model along with initial and boundary conditions as well as other relationships and constraints. This is followed by the adaptive homogenization section that discusses multiphase flow features that must be adequately resolved for an accurate solution. Further, this section also describes the three necessary ingredients of our upscaling approach. The solution algorithm section then outlines the workflow of the adaptive homogenization approach briefly touching upon the spatial and temporal discretization schemes employed, and the multiblock domain decomposition approach used for adaptive mesh refinement (AMR). Finally, the numerical results section provides comparison between fine scale solutions and adaptive homogenization approaches. A small subsection here is also dedicated to the speedups achieved by non-linear preconditioning necessary for the computational efficiency of our upscaling approach.

2 Model Formulation

We begin by describing an immiscible, two-phase, slightly compressible flow model in a porous medium. Although not restrictive, this model is chosen solely for its simplicity in explaining some of the details inherent to the adaptive homogenization approach presented in this work. Later, the adaptive homogenization section discusses how an accurate representation of fine scale flow features; using adaptive homogenization, leads to an accurate coarse scale solution. Future extensions of this work will encompass flow models with highly non-linear local equilibrium flow models such as equation of state (EOS) compositional flow as well as other non-linearities accounting for dynamic changes in fluid viscosity and surface tensions in the cases of polymer and chemical flooding, respectively. In this work, we restrict to the following simple model to draw out and explain some of the finer aspects of local numerical homogenization and adaptive mesh refinement (AMR).

2.1 Phase Conservation Equations

Consider a time interval $(0,T]$, along with a spatial domain, $\Omega \subset \mathbb{R}^d$, $d = 2$ or 3 with boundary $\partial\Omega$ and outward unit normal $\boldsymbol{n}$. The mass conservation equation for phase α is,

$$\frac{\partial(\phi\rho_\alpha S_\alpha)}{\partial t} + \nabla\cdot\rho_\alpha \boldsymbol{u}_\alpha = q_\alpha \text{ in } \Omega\times(0,T], \tag{1}$$

where ϕ is the rock porosity and ρ_α, S_α, $\mathbf{u}_\alpha$ and q_α are density, saturation, velocity and source/sink term, respectively of phase $\alpha =$ oil (o) or water (w). Further, the Darcy velocity for the phase α is given by,

$$\boldsymbol{u}_\alpha = -K\frac{k_{r\alpha}}{\mu_\alpha}(\nabla p_\alpha - \rho_\alpha \boldsymbol{g}) \text{ in } \Omega\times(0,T]. \tag{2}$$

Here, K and $\boldsymbol{g}$ are the rock permeability and gravitational constant, respectively. Further, $k_{r\alpha}$, μ_α and p_α are the relative permeability, viscosity and pressure of phase α.

2.2 Initial and Boundary Conditions

Although not restrictive, for the sake of simplicity we assume no flow boundary conditions.

$$\boldsymbol{u}_\alpha \cdot \boldsymbol{n} = 0 \text{ on } \partial\Omega \times (0,T] \tag{3}$$

$$p_\alpha = p_\alpha^0, \quad S_\alpha = S_\alpha^0, \text{ at } \Omega \times \{t = 0\} \tag{4}$$

Here, p_α^0, S_α^0 are the initial conditions for pressure and saturation of phase α.

2.3 Constraints and Other Conditions

The phase saturations S_α are constrained as,

$$\sum_\alpha S_\alpha = 1. \tag{5}$$

We assume capillary pressure and relative permeabilities to be continuous and monotonic functions of phase saturations. A precise description of the functional forms is avoided to maintain generality. However, the numerical results shown later use the Brooks-Corey [11] and van Genuchten [20] functional forms for relative permeability and capillary pressure, respectively.

$$p_c = f(S_o) = p_o - p_w \tag{6}$$

$$k_{r\alpha} = k_{r\alpha}(S_\alpha) \tag{7}$$

Further, both oil and water phase are assumed to slightly compressible with phase densities evaluated using

$$\rho_\alpha = \rho_{\alpha,ref} \exp\left[c_{f\alpha}(p_\alpha - p_{\alpha,ref})\right]. \tag{8}$$

Here, $c_{f\alpha}$ is the compressibility and $\rho_{\alpha,ref}$ is the density of phase α at the reference pressure $p_{\alpha,ref}$. We assume that the spatial rock porosity distribution is temporally invariant, or in other words the rock is assumed to be incompressible.

3 Adaptive Homogenization

Before we discuss the details of our adaptive homogenization approach, it is necessary here to discuss the nature of the partial differential equations (PDE) representing flow and transport in porous media. The phase mass conservation equations have a mixed parabolic-hyperbolic nature, parabolic in pressure and hyperbolic in saturation parabolic. This partial differential equation (PDE) is a diffusion equation in pressure variable for a given, temporally invariant, saturation distribution. The pressure solution has an infinite speed of propagation damped only by the compressibility of the fluid phases. In other words, if a source term is added anywhere in the domain Ω or if the boundary conditions are altered, the pressure solution changes instantaneously everywhere in the reservoir domain. This system further approaches a steady state solution at large times, wherein the pressure and hence velocities become temporally invariant. The dampening here refers to the delay in achieving a steady state from a given initial state and is entirely due to the compressible nature of the fluid. If the fluid phases are incompressible; or an absence of dampening, we arrive at the steady state solution instantaneously. For slightly compressible fluids, the time scale for achieving a steady

state pressure solution is much smaller (order of hours) than the usual reservoir simulation time scale (order of days). Therefore, an accurate pressure solution can be obtained without resolving the changes over the aforementioned fine time scale. Our previous findings [3] indicate that the numerical solution for single phase, slightly compressible, flow and component transport using our adaptive homogenization approach is in good agreement with fine scale solution.

However, the same cannot be said about advection time-scales (order of years), required for phase saturations (S_α) to achieve a steady state, that are much larger than reservoir simulation time-scale. The transport of a fluid phase due to advection is also represented by Eqn. (1) that is a hyperbolic PDE in saturation variable or a shock equation. One of the characteristic features of the saturation solution is the presence of a sharp front or shock which travels in the reservoir domain at a finite speed as shown by [12]. The front remains sharp in the absence of physical diffusion/dispersion, capillary pressure in our case, that otherwise causes smoothing. For the sake of simplicity of discussion; although not restrictive for our upscaling approach, we assume zero diffusion/dispersion. Another important feature to note is that the fluid phase velocity is dependent upon how accurately gradient of pressure and hence pressure is calculated. For layered permeability distribution; with stark contrast in permeability values, an accurate evaluation of this Darcy velocity is especially important since it differentiates high perm channels from its low perm counterparts. This permeability contrast, or layered distribution, at fine scale leads to spreading and mixing (different forms of dispersion) [22] at the coarse scale which must be captured for accurately predicting breakthrough times. Figure 2 shows three fine scale mechanisms contributing to coarse scale dispersion for a layered permeability medium at the fine scale. The blue color indicates the saturation front whereas the black and red arrows depict mixing induced by flow and capillary pressure differences, respectively across the layers at the fine scale. Please note that although not shown here for the sake of convenience, mixing due to capillary pressure differences along the layers also occurs. An interesting point to note here is that the two-scale homogenization theory describes that this coarse-scale dispersion is dependent on ratio of the fine to coarse length scales [4]. Or in other words, the scale dependency of dispersion can be derived starting from an established fine scale flow and transport model. In this sense, adaptive homogenization for multiphase flow shares common features with adaptive homogenization for single phase flow and tracer transport [3], wherein simple diffusion is now replaced by non-linear diffusion owing to capillary pressure.

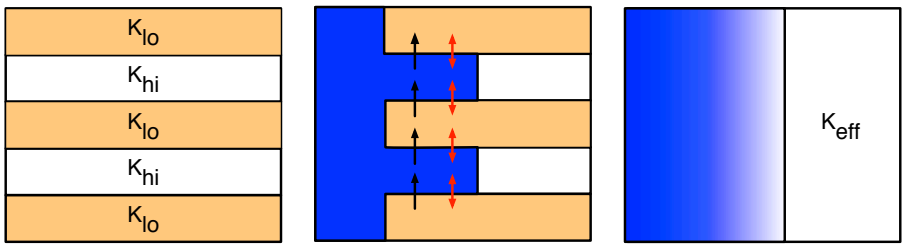

Figure 2: Fine scale permeability distribution (left), fine scale flow and transport (middle), and coarse scale flow and transport (right).

The adaptive homogenization approach presented here, captures all these aforementioned features by accurately resolving the saturation front while maintaining computational efficiency using

local numerical homogenization away from the front. The three key steps in our approach are:

1. Local numerical homogenization to obtain permeability values at the coarse scale by solving local unit-cell problems assuming single phase incompressible flow with periodic boundary conditions.

2. Evaluate an adaptivity criteria for identifying the location of the front and mark transient and non-transient regions.

3. Once the property data (permeability, porosity, etc.) is available at the coarse scale, an AMR scheme is used to solve the coupled transient (fine scale) and non-transient (coarse scale) flow and transport problems.

In the following subsections, we discuss the details of each of these aforementioned component that form our adaptive homogenization upscaling approach.

3.1 Local Numerical Homogenization

The local numerical homogenization step involves solving auxiliary problems over a subdomain Ω_i at a given fine scale to obtain an effective value of permeability, porosity or dispersion at a chosen coarse scale. Here, local is used to refer to the subdomains over which the auxiliary problems are solved using periodic boundary conditions for each subdomain. Figure 3 shows a schematic of the local numerical homogenization with the fine scale auxiliary problem (dotted red, left) to obtain coarse scale effective values (dotted red, right).

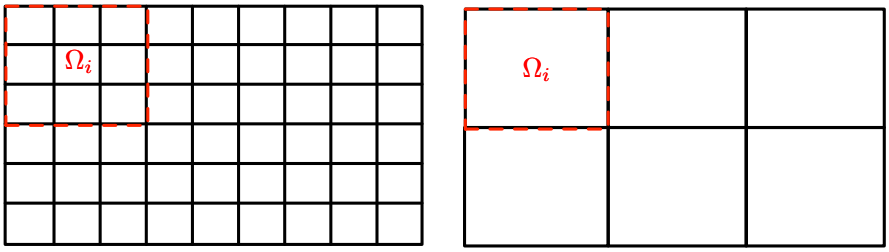

Figure 3: Schematic of local numerical homogenization to obtain coarse scale (right) parameters from fine scale (left).

The auxiliary problem for obtaining effective permeability values is given by,

$$\begin{aligned} -\nabla \cdot \left(K(y)\left(\nabla \chi^i + e_i\right)\right) = 0 \quad \text{in } Y \\ \chi^i \text{ is perodic in } Y. \end{aligned} \tag{9}$$

Here, χ^i is the auxiliary variable for the ith spatial dimension, i.e., $i = 1, 2, 3$ corresponding to the three spatial dimensions. Further, e_i is the unit vector in the ith spatial dimension (i.e., e_1 = [1 0 0], e_2 = [0 1 0], and e_3 = [0 0 1]). Once the above auxiliary problems; in the unknowns χ^i for each

spatial dimension i, are solved the effective permeability tensor at the coarse scale is then evaluated as,

$$\vec{w}^i(y) = -K(y)\left(\nabla\chi^i + e_i\right) \text{ for } i = 1,..,d$$
$$Q(y) = [\vec{w}^1(y), \vec{w}^2(y), .., \vec{w}^d(y)]$$
$$K^{eff} = -\langle Q \rangle = -\frac{1}{|Y|}\int_Y Q(y)dy$$

For further details regarding the derivation of these local auxiliary problems; using formal two-scale homogenization theory, the reader is referred to [3] and the citations therein. This calculation is performed once, as a preprocessing step, for a given fine scale permeability distribution and does not need to be recalculated unless the property distribution is altered. Note that this step remains unchanged even when the problem is changed from single phase [3] to the multiphase flow problem presented here rendering the local homogenization step process independence. Our speedup calculations; in the numerical results later, takes into account the computational overheads associated with solving these problems. The effective values obtained from this procedure results in a full-tensor permeability (non-zero off diagonal values) and therefore a multi-point flux scheme or an appropriate spatial discretization scheme must be used to accommodate the full-tensor requirement. However, in our calculations we neglected these off-diagonal values so that a simpler finite difference type discretization scheme can be used. Our numerical results indicate that this assumption did not result in substantial deviations in the tracer production histories for the adaptive solution as opposed to the fine scale solution.

3.1.1 Oversampling

Although the local numerical homogenization with non-overlapping subdomains provides good estimates for effective properties at the coarse scale, for some channelized cases this might result in loss of channel connectivity. This issue has been identified by several others; [17, 14] to cite a few, and has been addressed by using overlapping subdomains during the evaluation of multiscale basis. In this work, we use the same approach wherein subdomains are allowed to overlap over a predefined (or user specified) region. Figure 4 shows a schematic of oversampling for local numerical homogenization with overlapping subdomains. The effective properties are then evaluated by solving a local numerical homogenization over these extended subdomains.

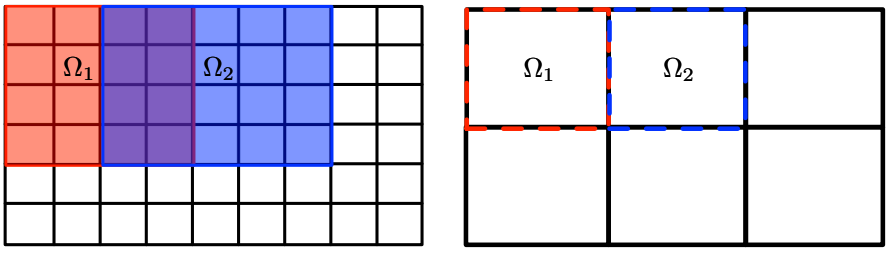

Figure 4: Oversampling for local numerical homogenization

We observe improvements in numerical solution accuracy of our adaptive approach; compared to the fine scale solution, for channelized permeability distributions with fine (or thin) high permeability streaks. This oversampling approach does not affect our overall computational efficiency since local numerical homogenization is performed only once prior to a numerical simulation for a given set of reservoir property distribution.

3.2 Adaptivity Criterion

We now require an indicator function to track the location of the saturation front in order to later perform a domain decomposition into transient and non-transient regions. An ad hoc criterion for identifying the location of the saturation front can be easily defined using a gradient in saturation between saturation at a given point in space and its nearest neighbor. One such criterion is using a maximum of absolute of difference between a saturation S at an element and its adjacent elements at the previous time step n. We define the neighboring elements collectively as, $\Omega_{neighbor}(x) = \{y : y \in E_j, |\partial E_i \cap \partial E_j| \neq \emptyset, \text{if } x \in E_i\}$. Then the adaptivity criteria can be written as,

$$\Omega_f = \left\{\mathbf{x} : \max|c^n(x) - c^n(y)| > \varepsilon_{adap} \quad \forall y \in \Omega_{neighbor}(x)\right\} \tag{10}$$

Here, E_i and E_j represent an element and its neighbors with ε_{adap} as the threshold value above which a domain is marked as a transient region. Please note that this type of adaptivity criterion has been used by others [1] to reduce computational costs in a similar sense. However, the computational speedup obtained in the former is not clear. Such criteria have been used in the past for different problems as well. For example, in compositional flow modeling [24], the local equilibrium computations (flash calculations) are performed based upon the identification of a spatial transient region where a given fluid composition was unstable at a previous timestep.

3.3 Adaptive Mesh Refinement

Based upon the above criteria we divide the domain (Ω) into non-overlapping, transient (Ω_f) and non-transient (Ω_c) subdomains to solve flow and transport problems at the fine and coarse scales, respectively. Figure 5 shows a schematic of the domain decomposition approach used here. In what follows, coarse and non-transient, and fine and transient can be used interchangeably to refer to a subdomain. The coarse and fine subdomain problems are then coupled at the interface using the EVMFEM spatial discretization described in [27]. The EV MFE method is known to be strongly mass conservative at the interface between fine and coarse domains. Further, this scheme has been used previously; as a multiblock domain decomposition approach, for a number of fluid flow and transport problems [26] including EOS compositional flow. This adaptive homogenization approach has also been used for upscaling single phase, slightly compressible flow, and tracer transport in [3]. Here, the EV MFE was used as the multiblock, domain decomposition approach similar to its usage in this work.

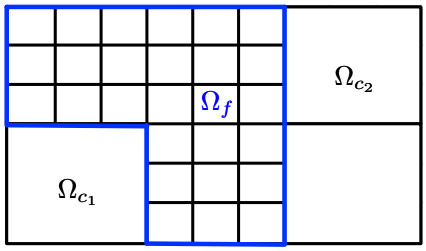

Figure 5: Schematic of adaptive mesh refinement with coarse (Ω_c) and fine (Ω_f) domains.

We briefly discuss, the fully coupled, discrete variational formulation of the two phase flow problem using a backward Euler scheme for time and EV MFEM for spatial discretization. Let oil phase pressure (p_o), saturation (S_o), and Darcy ($\mathbf{u}_\alpha$) and auxiliary fluxes ($\tilde{\mathbf{u}}_\alpha$) to be the primary unknowns. Note that after Newton linearization, the fluxes are eliminated from the linear equations resulting in a linear system in pressure (p_o) and saturation (S_o) unknowns. The variational problem is given by: Find $\mathbf{u}_{\alpha,h} \in L^2\left(J, \mathbf{V}_h^{*,0}\right)$, $p_{o,h} \in H^1(J, W_h)$, $\tilde{\mathbf{u}}_{\alpha,h} \in L^2\left(J, \mathbf{V}_h^{*,0}\right)$ and $S_{o,h} \in H^1(J, W_h)$ such that,

$$
\left.
\begin{aligned}
&\left(\tfrac{\partial}{\partial t}\phi\rho_o(p_{o,h})S_{o,h}, w_h\right)_\Omega + (\nabla\cdot\rho_o(p_{o,h})\mathbf{u}_{o,h}, w_h)_\Omega = (q_o, w_h)_\Omega \\
&\left(\tfrac{\partial}{\partial t}\phi\rho_w(p_{o,h}, S_{o,h})(1-S_{o,h}), w_h\right)_\Omega + (\nabla\cdot\rho_w(p_{o,h})\mathbf{u}_{w,h}, w_h)_\Omega \quad = (q_w, w_h)_\Omega
\end{aligned}
\right\} \quad \forall\, w_h \in W_h
$$

$$
\left.
\begin{aligned}
&\left(K^{-1}\tilde{\mathbf{u}}_{o,h}, \mathbf{v}_h\right)_\Omega - (p_{o,h}, \nabla\cdot\mathbf{v}_h)_\Omega - (\rho_o(p_{o,h})\vec{g}, \mathbf{v}_h)_\Omega = 0 \\
&(\lambda_o\tilde{\mathbf{u}}_{o,h}, \mathbf{v}_h)_\Omega = (\mathbf{u}_{o,h}, \mathbf{v}_h)_\Omega \\
&\left(K^{-1}\tilde{\mathbf{u}}_{w,h}, \mathbf{v}_h\right)_\Omega - (p_{o,h}, \nabla\cdot\mathbf{v}_h)_\Omega + (p_c(S_{o,h}), \nabla\cdot\mathbf{v}_h)_\Omega - (\rho_w(p_{o,h}, S_{o,h})\vec{g}, \mathbf{v}_h)_\Omega = 0 \\
&(\lambda_w\tilde{\mathbf{u}}_{w,h}, \mathbf{v}_h)_\Omega = (\mathbf{u}_{w,h}, \mathbf{v}_h)_\Omega
\end{aligned}
\right\} \quad \forall\, \mathbf{v}_h \in \mathbf{V}_h^{*,0}
\tag{11}
$$

Here, $J = (0, T]$ is the time domain, $W_h(\Omega) = \{w \in L^2(\Omega) : w|_E \in W_h(E), \forall E \in \mathscr{T}_h\}$ and $\mathbf{V}_h^{*,0} \equiv \mathbf{V}_h^* \cap \{\mathbf{v} : \mathbf{v}\cdot\nu = 0 \text{ on } \partial\Omega\}$ are the discrete spaces for pressure/saturation and velocity degrees of freedom, respectively. The pressure and saturation degrees of freedom are defined as piecewise constants on the elements whereas the flux (or velocity) degrees of freedom are piecewise constants on the element edges. $\mathbf{V}_h^*$ is the discrete enhanced velocity space as described in [27].

4 Solution Algorithm

In this section, we discuss the numerical solution algorithm with a brief description of spatial and temporal discretizations employed. We assume that the oil phase pressure p_o and saturation S_o are the primary unknowns to form the non-linear system of algebraic equations representing the weak form of the two-phase flow model formulation. The lowest order (RT0) mixed finite element method [5] ; equivalent to the finite difference scheme, is used for spatial discretization with a

backward Euler scheme for temporal discretization. A Newton linearization is then performed to obtain a linear system of algebraic equations hence resulting in a fully implicit solution scheme.

Algorithm 1 Workflow for adaptive numerical homogenization

Solve unit-cell problems, Eqns. (9), on subdomains (Ω_i) using fine scale parameters to obtain coarse scale parameters for the entire domain ($\Omega = \cup\Omega_i$, see Figure 3).

while $t_n \leq T$ **do**

Identify transient (Ω_f) and non transient (Ω_c) regions using adaptivity criteria Eqn. (10) and p_o, S_o at t_n ($\Omega_f \cup \Omega_c = \Omega$).

Mass conservative initialization of primary unknowns:

1. Reconstruct primary unknowns $p_o^{n+1,0}, S_o^{n+1,0}$ for the fine scale transient region (Ω_f).
2. Project primary unknowns $p_o^{n+1,0}, S_o^{n+1,0}$ for the coarse scale non-transient region (Ω_c).

while $max(\vec{R}_{nl}) > \varepsilon_{nl}$ **do**

1. Use fine and coarse scale parameters in the transient (Ω_f) and non-transient (Ω_c) regions, respectively.
2. Use enhanced velocity (EV) scheme to couple coarse and fine subdomains.
3. Solve linearized, algebraic system for the coupled flow and transport problem to obtain a Newton update $p_o^{n+1,k+1}, S_o^{n+1,k+1}$.

$k := k+1$

end

$t_{n+1} = t_n + \Delta t$, $n := n+1$

end

Algorithm 1 presents the solution algorithm for the adaptive homogenization approach. Here, n and k are the time and non-linear iteration counter, t_n and t_{n+1} are the current and next time, Δt current time-step size, T the final time, $max(\vec{R}_{nl})$ the max norm of the non-linear residual vector, and ε_{nl} the non-linear tolerance. The adaptivity criteria (10) is evaluated at the coarse scale; for each time step, to identify the transient region for the next time step. Once identified the reservoir domain is divided into fine (Ω_f) and coarse Ω_c subdomains. A fully coupled, monolithic construction of the multiblock domain decomposition approach EV MFEM is then used for coupling non-matching coarse and fine subdomains. The coupled monolithic construction is an improvement over the previous implementations of the EV MFEM [27, 26] approach where the interface contributions are neglected. This approach was also used for upscaling single-phase flow and tracer transport earlier by [3]. The non-linear iterations are performed until the max norm ($max(\vec{R}_{nl})$) satisfies a desired tolerance (ε_{nl}) corresponding to the error in phase mass conservation equations.

4.1 Projection/Reconstruction

Prior to each new timestep solve, a projection (or reconstruction) of the previous timestep, fine (or coarse) scale unknowns onto the coarse (or fine) scale is performed if the adaptivity criteria indicates a change from coarse to fine or vice versa. The reconstruction is performed by copying previous coarse scale unknown into all the new fine scale unknowns. Since pressure (p_o) and saturation (S_o) are intensive properties this operation remains mass conservative. On the other hand, a local solve is necessary for a mass conservative projection of fine grid unknowns onto a coarse grid given by the system of equations,

$$\begin{aligned} \sum_{E_i} |E_i| \rho_\alpha(p_{o,i}) S_{\alpha,i} = |E| \rho_\alpha(p_{o,avg}) S_{\alpha,avg} \ , \alpha = o,\ w, \\ \sum_{\alpha} S_{\alpha,avg} = 1. \end{aligned} \tag{12}$$

These three equations are solved locally for the unknowns $p_{o,avg}$, $S_{o,avg}$ or the projection of the known fine grid values of $p_{o,i}$, $S_{o,i}$ onto the coarse grid . The phase densities are evaluated using the same functional form, Eqn. (8), at both fine and coarse scales. Here, $|E_i|$ and $|E|$ denote the measure (or volumes) of the fine and coarse scale elements. An important point to note here is that this conservative projection is valid for a fully compressible fluid description such as the immiscible gas phase as well. It is easy to check that for incompressible fluids, this system reduces to a volume-weighted, arithmetic mean of fine scale unknowns (p_o, S_o). The computational overhead due to this mass conservative, local projection operation is quite small and as such does not affect the overall computational efficiency of our upscaling scheme.

4.2 Non-linear Preconditioning

The adaptive mesh refinement and consequently the coupled fine and coarse grid subdomain problem introduce convergence issues in the non-linear (or Newton) solve. In our numerical simulation, we observed that using a fine grid; with given heterogeneous parameters, for the entire reservoir domain resulted in substantial increase in non-linear iterations compared to a coarse grid; with calculated effective parameters. In fact, for some cases the non-linear iterations did not converge for the fine grid with large time-step sizes (order of days) requiring smaller time-step sizes. The coupled fine and coarse grid also ran into similar convergence issues (large number of non-linear iterations) with same time-step sizes indicating that the initial estimate of the unknowns p_o, S_o after projection/reconstruction operation is not sufficient. This results in additional computational overheads due to increased non-linear iterations or worse restrictive time-step sizes originating from the use of a fine grid during AMR step. Since the convergence of Newton method is dependent on the proximity of the initial estimate (or guess) to the final solution, it is necessary to devise a computational cost-efficient method for generating these initial estimates. As a part of this work, we also developed a non-linear preconditioning technique to improve Newton convergence based upon solving an approximate, linear multiphase flow system prior to the non-linear, two-phase flow system solve.

For the non-linear two-phase, slightly compressible, oil-water flow system an approximate, linear, multiphase flow system is generated by replacing the relative permeability, Eqn. (7), and capilliary pressure , Eqn. (6) curves; which are non-linear functions of saturations, with linear functions. Further, the phase densities are taken to be constant instead of as a non-linear function of phase pressures, Eqn. (8). Note that in the above treatment it is necessary that the end points of the

relative permeability and capillary pressure curves be preserved even in the linear approximation. Once the aforementioned procedure is performed, the resulting system given us the approximate linear form of the non-linear, two-phase flow system. This linear system is then solved for a loose Newton tolerance (order of 10^{-2}) to obtain a preconditioner for the fully non-linear system. After preconditioning, the non-linear system is solved with a tight Newton tolerance (order of 10^{-8}) to obtain the solution; for a given timestep, for the actual multiphase flow system.

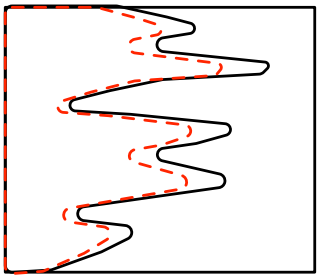

Figure 6: Non-linear preconditioning: proximity of linear and non-linear multiphase systems.

Figure 6 provides a rough description of the assistance provided by this non-linear preconditioner during the actual non-linear solve. The saturation front is moving from left to right in a heterogeneous porous medium resulting in an uneven front. The red dotted and black lines show the approximate and actual solutions obtained, respectively by solving the two systems in succession. In our numerical simulations, we observed that the number of total non-linear iterations (including preconditioning and non-linear solve) reduced from 30 (or more) to 12 (or less) for a given time-step size (order of days). Furthermore, we were consistently able to take time-step sizes of 1 day; for all our numerical simulations, that is otherwise restricted to atmost 0.25 days in the absence of the proposed non-linear preconditioner. The numerical results section below contains a brief description of the speedups obtained due this non-linear preconditioning. A variant of the same technique can also be used to precondition air-water or black-oil type multiphase flow systems. Please note that this non-linear preconditioning approach can be generalized by borrowing notions from acceleration techniques such as the forcing function approach [18, 15]. Here, the linear solver tolerance is tightened as the non-linear solver converges to a desired non-linear tolerance to reduce computational overheads. The non-linear preconditioning approach presented here begins with an approximate linear system that gradually approaches the actual non-linear system, as the non-linear solver approaches convergence. The choice of the approximate linear system and the approach to the actual non-linear system is made based upon arguments on the continuity of the non-linear functions. We restrict this discussion on non-linear preconditioning to the problem at hand; the two-phase flow system, with an intent to generalize this approach in the near future.

5 Numerical Results

In this section, we present numerical experiments beginning with verification cases for numerical homogenization and AMR using periodic and homogeneous reservoir properties, respectively for the two cases. Next we demonstrate the capability of our adaptive homogenization approach using

reservoir property description from different horizontal layers of the 10^{th} SPE comparative project for upscaling approaches [13]. We specifically rely upon two layers of the SPE10 project: (1) layer 20 with a near Gaussian distribution of permeability, and (2) layer 38 with layered or highly channelized permeability distribution. These contrasting cases are aimed to test the solution accuracy and computational efficiency of our adaptive homogenization approach compared to a fine scale solve over the entire reservoir domain. The reservoir domain is 220ft$\times$60ft with coarse and fine scale grid discretizations of 22×6 and 220×60, respectively. The coarse and fine grid elements are consequently 10ft$\times$10ft and 1ft$\times$1ft. The fluid and reservoir properties are mostly taken from the SPE10 dataset with minor modifications to oil phase compressibility to fit the two-phase flow model formulation. The oil and water phase compressibility is taken to be 1×10^{-4} and 3×10^{-6} psi^{-1} , respectively. Further the fluid viscosities is assumed to be 3 and 1 cP for the oil and water phases, respectively. Additionally, a Brook's Corey model, Eqn. (13), is considered for the two-phase relative permeabilities with endpoints S_{or} = S_{wirr} = 0.2 and $k^0_{ro} = k^0_{rw} = 1.0$, and model exponents $n_o = n_w = 2$, as suggested in the SPE10 dataset.

$$\begin{aligned} k_{rw} &= k^0_{rw}\left(\frac{S_w - S_{wirr}}{(1 - S_{or} - S_{wirr}}\right)^{n_w} \\ k_{ro} &= k^0_{ro}\left(\frac{S_o - S_{or}}{(1 - S_{or} - S_{wirr}}\right)^{n_o} \end{aligned} \tag{13}$$

Although the capillary pressure is assumed to be identically zero in the original dataset, we assume a van Genuchten capillary pressure model, Eqn. (14) to demonstrate the capabilities of our upscaling approach.

$$p_c(S_w) = a\left[(S_w - S_{wirr})^{-1/b} - 1\right]^{1/c} \tag{14}$$

In all of the following numerical cases, the initial reservoir pressure and saturation are taken to be 1000 psi and 0.2, respectively. Further, the injection well is water-rate specified at 2 STB/-day whereas the production well is pressure specified at 1000 psi. All numerical simulations are carried out for a total of 200 days with continuous water injection. Please note that although a homogeneous dataset is provided in SPE10 data for relative permeability and capillary pressure, our upscaling approach is not restrictive in this sense. In fact, for such heterogeneities an average relative permeability and capillary pressure can be obtained at the coarse scale; following the two-scale homogenization work of [10]. However, we do not need to evaluate these effective functions at the coarse scale since we are resolving fine scale features at the front using AMR. Our adaptive homogenization only requires that the effective endpoints of relative permeability be evaluated at the coarse scale such that,

$$\begin{aligned} |E|a_E &= \sum_i |E_i| a_{E_i}, \\ a &= S_{or},\ S_{wirr},\ k^0_{r\alpha}. \end{aligned} \tag{15}$$

Here, 'a' is used to denote the end-points of the relative permeability model. A consistent, coarse scale capillary pressure is then given by,

$$|E|p_c(1 - S_{or}\big|_E) = \sum_i |E_i| p_c(1 - S_{or}\big|_{E_i}). \tag{16}$$

This intuitively also makes sense since different rock types result in different irreducible water and residual oil saturations at the fine scale that must be captured at the coarse scale for accuracy.

Again these computations are also performed once prior to the simulation run and remain unchanged unless the fine scale, relative permeability and capillary pressure data is altered. Figure 7 shows the relative permeability and capillary pressure curves; as function of water phase saturation, for the oil and water phases. As mentioned earlier, the SPE10 dataset was used to populate the model parameters for the relative permeability curves.

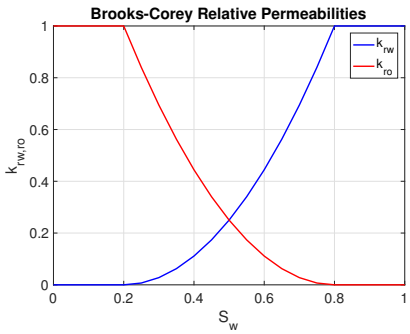

Figure 7: Relative permeability (from SPE10 dataset) and capillary pressure curves (augmentation).

5.1 Homogeneous Verification Case

We verify the adaptivity criteria and AMR using a homogeneous permeability of distribution of 50mD. Figure 8 shows the saturation profile after hundred days of continuous water injection. As can be easily seen from these figures the saturation profiles for the fine and adaptive approaches are in excellent agreement.

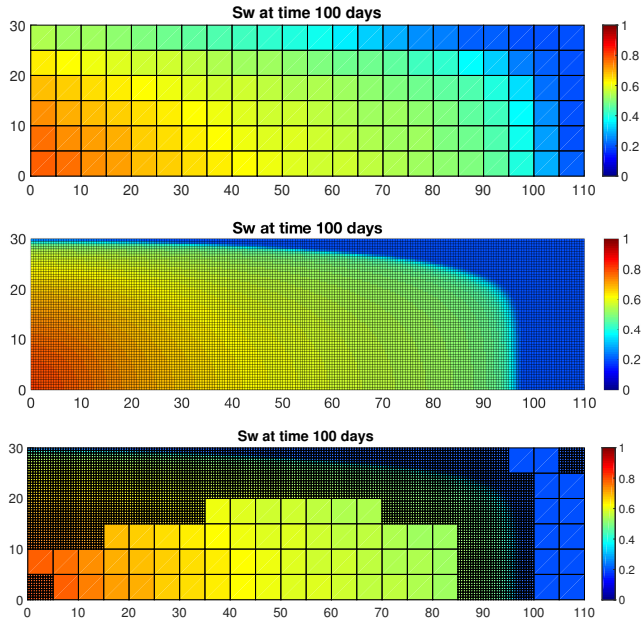

Figure 8: Saturation profiles after 100 days for coarse (top), fine (middle), and adaptive (bottom) appraoches.

Figures 9 and 10 further show the oil rate and cumulative oil at the production well, respectively. These results further bolster the fact that the AMR with the proposed adaptivity criteria provides an accurate solution when compared against the fine scale solution. The coarse scale solution deviates mildly from the other two set of results due to numerical diffusion introduced by the upwinding scheme and coarse grid discretization. The AMR is able to curtail the numerical diffusion introduced by upwinding at the saturation front by using a dynamic fine grid around the saturation front.

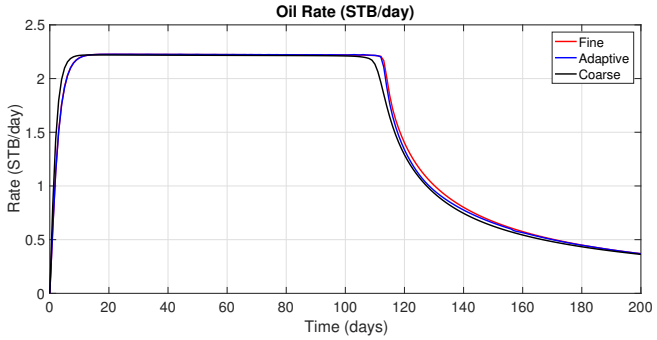

Figure 9: Oil rate at production well (STB/day).

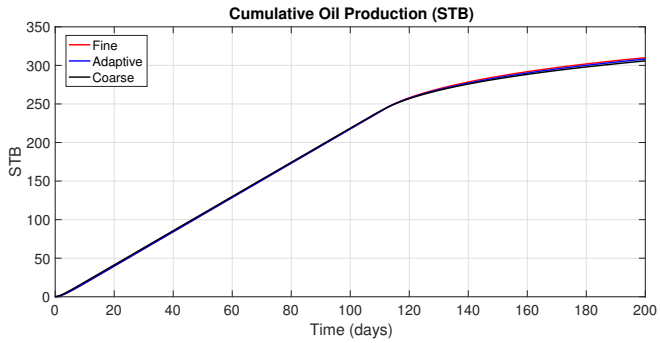

Figure 10: Cumulative oil production (STB)

5.2 Gaussian Permeability Distribution

For this numerical test, we use layer 20 of the SPE10 dataset that has a relatively Gaussian distribution of permeability. Figure 11 shows fine scale permeability distribution; extracted from the dataset, and coarse scale distribution obtained after numerical homogenization. As discussed earlier, this numerical homogenization step to obtain effective properties at the coarse scale is only performed once and does effect the overall computational efficiency.

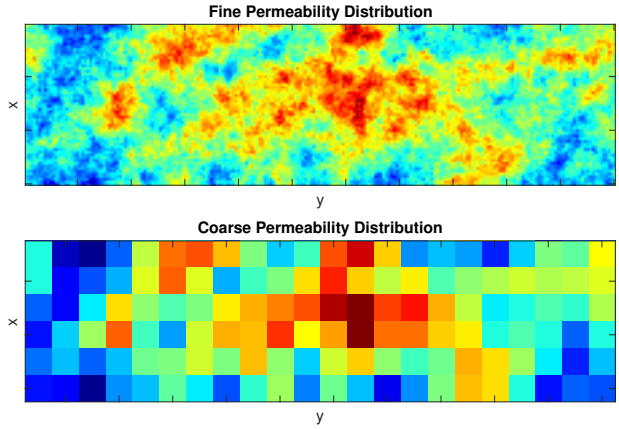

Figure 11: Permeability distribution at fine (top) and coarse (bottom) scale from SPE10 layer 20.

Figure 12 shows the saturation profile after 50 days for the coarse, fine, and adaptive approaches. It is clear from these figures that saturation fronts are captured almost as accurately as the fine scale solution at substantially less computational cost. This is achieved by solving the fine scale problem only in reservoir subdomains where changes in saturation are large; as identified by our adaptivity criteria.

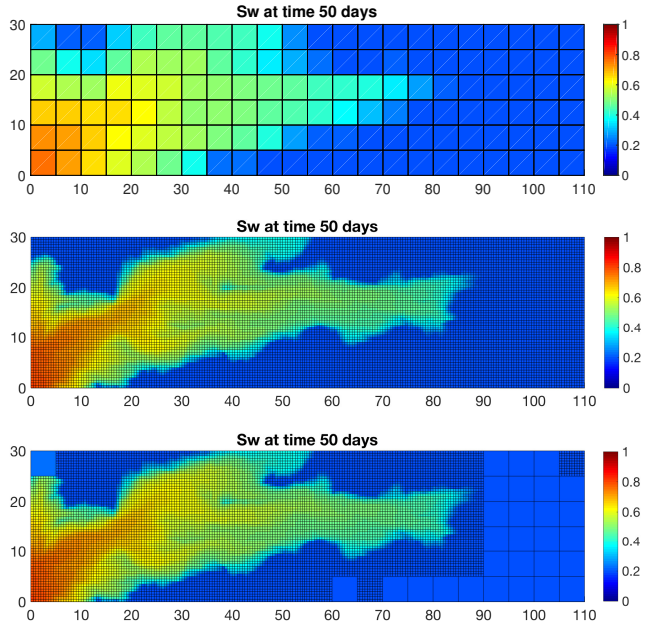

Figure 12: Saturation profiles after 50 days for coarse (top), fine (middle), and adaptive (bottom) appraoches.

Figures 13 and 14 show the oil rate and cumulative oil at the production well. These figures clearly show that the adaptive approach is again in excellent agreement with the fine scale solution for the Gaussian permeability distribution under consideration. Again, this is more or less expected since the permeability distribution is Gaussian in nature and therefore has some ergodicity; or periodic properties in a statistical paradigm. Therefore the basic assumptions of two-scale homogenization theory and consequently local numerical homogenization are inherently valid.

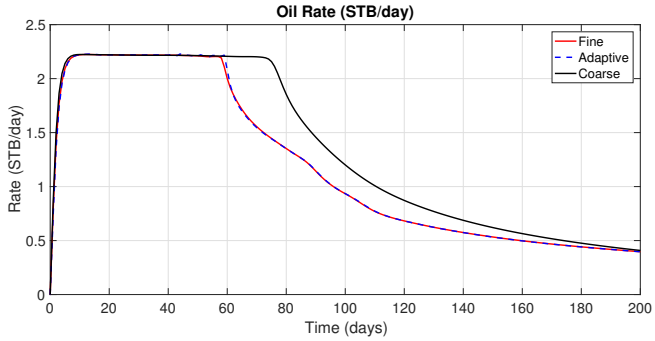

Figure 13: Oil rate at production well (STB/day) for layer 20 of SPE10.

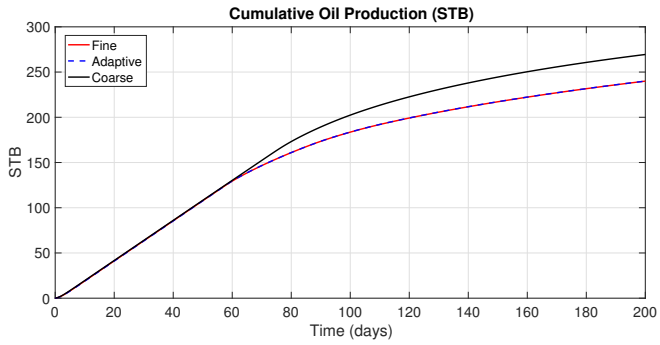

Figure 14: Cumulative oil production (STB) for layer 20 of SPE10.

5.3 Channelized Permeability Distribution

Next, we consider layer 38 of the SPE10 dataset that has a channelized or layered permeability distribution with stark contrast in permeability values. Figure 15 shows fine scale permeability distribution and coarse scale distribution obtained after numerical homogenization; similar to the previous numerical test case. This figure clearly shows that channels connectivity is lost in the coarse scale permeability distribution obtained from local numerical homogenization.

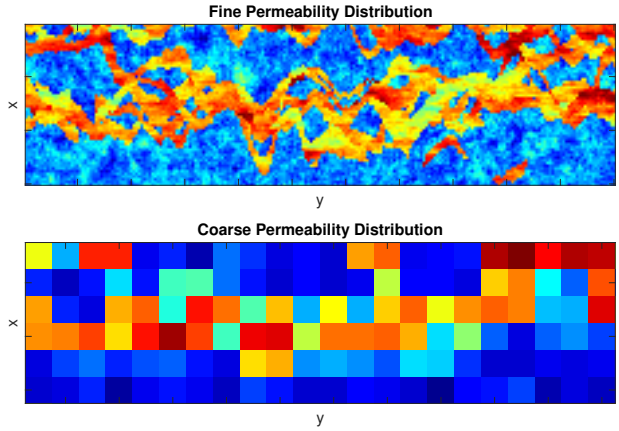

Figure 15: Permeability distribution at fine (top) and coarse (bottom) scale from SPE10 layer 38.

We are able to recover connectivity using oversampling to some extent however, we still observe a substantial deviation in solution accuracy for the coarse scale. However, our adaptive homogenization approach is still able to recover fine scale features as can be seen from the saturation profile in Figure 16.

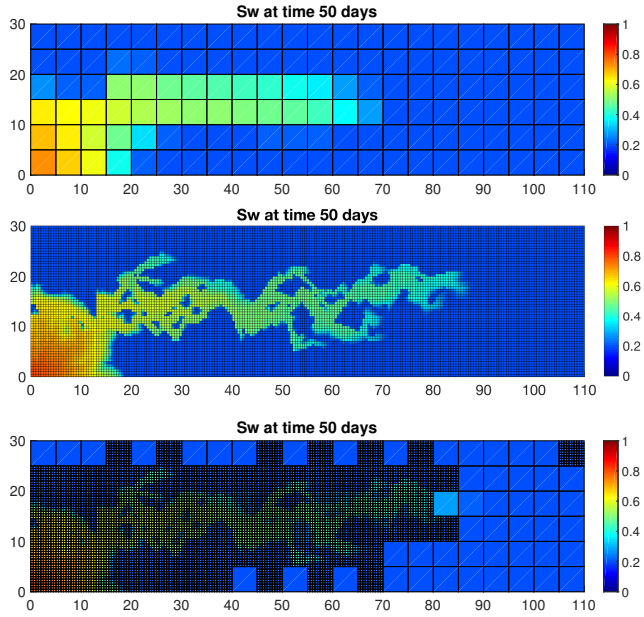

Figure 16: Saturation profiles after 50 days for coarse (top), fine (middle), and adaptive (bottom) appraoches.

Figures 17 and 18 show the oil rate and cumulative oil at the production well. The deviation of the oil rate for the adaptive case (spikes) can be improved by tightening the adaptive criteria, however this results in additional computational overheads. Since the cumulative oil production is already a good match we did not consider this aforementioned approach to resolve the oil-rates better.

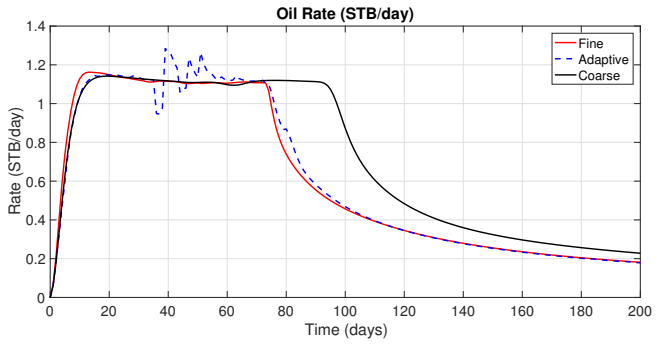

Figure 17: Oil rate at production well (STB/day) for layer 38 of SPE10.

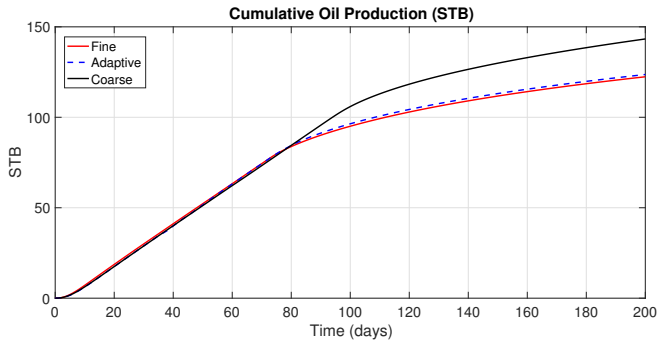

Figure 18: Cumulative oil production (STB) for layer 38 of SPE10.

6 Conclusions

A novel adaptive numerical homogenization approach is presented that relies upon identifying characteristic flow features; such as the saturation front, and resolving them at the fine scale for accuracy. The computational efficiency is achieved by solving a coarse scale problem away from the saturation front with effective coefficients; obtained from one time local numerical homogenization for a given reservoir property distribution, at the coarse scale. An oversampling technique for the local numerical homogenization step preserves connectivity of channels; across coarse subdomains, in a layered permeability medium. Further, a non-linear preconditioning approach was developed to reduce the number of non-linear iterations improving the computational efficiency of the overall approach for a multiphase flow system. The numerical results indicate that the solutions obtained using our adaptive homogenization approach are in good agreement with the fine scale solutions. The breakthrough times and production histories are predicted more accurately compared to a purely coarse scale; using local numerical homogenization without AMR, solve. We obtain a speedup of approximately 4 times for all our numerical test cases since the saturation front; where a fine scale solution is required, occupies only a small subdomain of the entire reservoir. Further speedups can be obtained by using a loose adaptivity criteria at the cost of solution accuracy. This approach can be easily extended to black-oil, compositional (gas and chemical flooding), and reactive flow type systems with a some modifications in local numerical homogenization and non-linear preconditioning steps. As mentioned previously, the effective equations; using two-scale homogenization, for different flow models share common workflow elements that do not change with the flow model under consideration. Thus adaptive homogenization is a general upscaling framework with a certain degree of process independence.

7 Acknowledgements

This research was funded by DOE NETL grant DE-FE0023314. The authors would like to extend a special thanks to Prof. Hans van Duijn (Rector Magnificus of Eindhoven University of Technology) for his help on two-scale homogenization theory. We would also like to acknowledge the Center for Subsurface Modeling industrial affiliates for their continuing support.

8 Nomenclature

$\Omega =$ reservoir domain

$\Omega_c =$ coarse subdomain

$\Omega_f =$ fine subdomain

$\partial\Omega =$ reservoir flow boundary

$\phi =$ porosity

ref $=$ standard condition for density evaluation

$\alpha =$ oil (o) or water (w) phase

$S_\alpha =$ saturation of phase 'α'

$S_{\alpha,avg} =$ average saturation of phase 'α' at the coarse scale

$S_{wirr} =$ irreducible water saturation

$S_{or} =$ residual oil saturation

$p_\alpha =$ pressure of phase 'α'

$p_{\alpha,avg} =$ average pressure of phase 'α' at the coarse scale

$p_c =$ capillary pressure

$\rho_\alpha =$ density of phase 'α'

$p_\alpha^0 =$ initial condition for pressure of phase 'α'

$S_\alpha^0 =$ initial condition for saturation of phase 'α'

$\boldsymbol{u}_\alpha =$ Darcy flux of phase 'α'

$\nu_\alpha =$ viscosity of phase 'α'

$c_\alpha =$ compressibility of phase 'α'

$kr_\alpha =$ relative permeability of phase 'α'

$kr_\alpha^0, n_\alpha =$ Brooks Corey relative permeability parameter for phase'α'

$q_\alpha =$ source or sink term for phase 'α'

$K =$ absolute permeability

$K^{eff} =$ effective value of absolute permeability

$S_{wirr} =$ Irreducible water saturation

$S_{or} =$ Residual oil saturation

$w^i(y) =$ Auxiliary velocity in ith spatial dimension

$Q(y) =$ Auxiliary velocity tensor

$a, b, c =$ Van Genuchten model parameters

$|E_i| =$ measure (or volume) of the fine scale element E_i

$|E| =$ measure (or volume) of the coarse scale element E

References

[1] Jørg E Aarnes and Yalchin Efendiev. An adaptive multiscale method for simulation of fluid flow in heterogeneous porous media. *Multiscale Modeling & Simulation*, 5(3):918–939, 2006.

[2] Grégoire Allaire. Homogenization and two-scale convergence. *SIAM Journal on Mathematical Analysis*, 23(6):1482–1518, 1992.

[3] Yerlan Amanbek, Gurpreet Singh, Mary F. Wheeler, and Hans van Duijn. Adaptive numerical homogenization for upscaling single phase flow and transport. *ICES Report*, 12(17), 2017.

[4] Brahim Amaziane, Alain Bourgeat, and Mladen Jurak. Effective macrodiffusion in solute transport through heterogeneous porous media. *Multiscale Modeling & Simulation*, 5(1):184–204, 2006.

[5] T. Arbogast, M.F. Wheeler, and I. Yotov. Mixed finite elements for elliptic problems with tensor coefficients as cell-centered finite differences. *SIAM J. Numer. Anal.*, 32(2):828–852, 1997.

[6] Todd Arbogast. *Mixed Multiscale Methods for Heterogeneous Elliptic Problems*, pages 243–283. Springer Berlin Heidelberg, Berlin, Heidelberg, 2012.

[7] Todd Arbogast, Gergina Pencheva, Mary F Wheeler, and Ivan Yotov. A multiscale mortar mixed finite element method. *Multiscale Modeling & Simulation*, 6(1):319–346, 2007.

[8] Jacob Bear. Dynamics of fluids in porous media. *Textbook*, 1972.

[9] Alain Bensoussan, Jacques-Louis Lions, and George Papanicolaou. *Asymptotic analysis for periodic structures*, volume 5. North-Holland Publishing Company Amsterdam, 1978.

[10] A. Bourgeat, M. Jurak, and A. L. Piatnitski. Averaging a transport equation with small diffusion and oscillating velocity. *Mathematical Methods in the Applied Sciences*, 26(2):95–117, 2003.

[11] R.H. Brooks and A.T. Corey. Hydraulic properties of porous media. *Hydrology Papers No. 3*, 26(2), 1964.

[12] S.E. Buckley and M.C. Leverett. Mechanism of fluid displacement in sands. *SPE Journal*, 146(01), 1942.

[13] M. A. Christie and M. J. Blunt. Tenth spe comparative solution project: A comparison of upscaling techniques. *SPE Reservoir Evaluation and Engineering*, 4(04), 2001.

[14] Eric Chung, Yalchin Efendiev, and Thomas Y Hou. Adaptive multiscale model reduction with generalized multiscale finite element methods. *Journal of Computational Physics*, 320:69–95, 2016.

[15] C. N. Dawson, H. Klie, M. F. Wheeler, and C. S. Woodward. A parallel, implicit cell-centered method for two-phase flow with a preconditioned newton-krylov solver. *Computational Geosciences*, 1(3):215–249, 1998.

[16] Louis J Durlofsky. Upscaling of geocellular models for reservoir flow simulation: A review of recent progress. In *7 th International Forum on Reservoir Simulation*. Citeseer, 2003.

[17] Yalchin Efendiev and Thomas Y Hou. *Multiscale finite element methods: theory and applications*, volume 4. Springer Science & Business Media, 2009.

[18] S. C. Eisenstat and H. F. Walker. Globally convergent inexact newton methods. *SIAM Journal of Optimization*, 4(2):393–422, 1994.

[19] C. L. Farmer. Upscaling: a review. *International Journal for Numerical Methods in Fluids*, 40(1):63–78, 2002.

[20] Van Genuchten. A closed-form equation for predicting the hydraulic conductivity of unsaturated soils. *Soil Science Society of America Journal*, 44(5):892–898, 1980.

[21] Vasilii Vasil'evich Jikov, Sergei M Kozlov, and Olga Arsen'evna Oleinik. *Homogenization of differential operators and integral functionals*. Springer Science & Business Media, 2012.

[22] Abraham K. John. *Dispersion in Large Scale Permeable Media*. PhD thesis, The University of Texas at Austin, 2008.

[23] Andro Mikelić, Vincent Devigne, and CJ Van Duijn. Rigorous upscaling of the reactive flow through a pore, under dominant peclet and damkohler numbers. *SIAM journal on mathematical analysis*, 38(4):1262–1287, 2006.

[24] Gurpreet Singh and Mary F. Wheeler. Compositional flow modeling using a multi-point flux mixed finite element method. *Computational Geosciences*, 20(3):421–435, 2016.

[25] Reza Tavakoli, Hongkyu Yoon, Mojdeh Delshad, Ahmed H. ElSheikh, Mary F. Wheeler, and Bill W. Arnold. Comparison of ensemble filtering algorithms and null-space monte carlo for parameter estimation and uncertainty quantification using co2 sequestration data. *Water Resources Research*, 49(12):8108–8127, 2013.

[26] Sunil G Thomas and Mary F Wheeler. Enhanced velocity mixed finite element methods for modeling coupled flow and transport on non-matching multiblock grids. *Computational Geosciences*, 15(4):605–625, 2011.

[27] John A Wheeler, Mary F Wheeler, and Ivan Yotov. Enhanced velocity mixed finite element methods for flow in multiblock domains. *Computational Geosciences*, 6(3-4):315–332, 2002.

[28] Xiao-Hui Wu, Y Efendiev, and Thomas Y Hou. Analysis of upscaling absolute permeability. *Discrete and Continuous Dynamical Systems Series B*, 2(2):185–204, 2002.